Residues from the Fundão dam accident in Brazil and their effects on photosynthetic efficiency of two restinga plant species

Namir Gabriely Matos Lopes[1*]; Eliemar Campostrini[2]; Marcel Giovanni Costa França[3]; Diolina Moura Silva[1]

[1] Departamento de Biologia Vegetal, Universidade Federal do Espírito Santo, 29075-910, Vitória, ES, Brazil

[2]Setor Fisiologia Vegetal, Centro de Ciências e Tecnologias Agropecuárias, Universidade Estadual Norte Fluminense (UENF), Darcy Ribeiro, Brazil

[3]Departamento de Botânica, Universidade Federal de Minas Gerais, Av. Antônio Carlos, 6627, Pampulha, Belo Horizonte, MG, Brazil

* Corresponding author at: Departamento de Biologia Vegetal, Universidade Federal do Espírito Santo, 29075-910, Vitória, ES, Brazil. E-mail address: namirmatos@gmail.com (NGM Lopes).

Abstract

In 2015, a breach in the Fundão Dam in Mariana (Minas Gerais State, Brazil) resulted in the release of contaminated tailings into the Doce River basin. This accident increased the concentrations of arsenic (As), lead (Pb), cadmium (Cd), vanadium (V), and manganese (Mn) in the soil, posing a potential hazard to the physiology of native species. Therefore, this study aimed to assess whether chlorophyll *a* fluorescence (ChlF) in *Allagoptera arenaria* and *Guapira pernambucensis* changed following this accident when tested under different precipitation regimes in relation to soil properties, and heavy metal absorption. Our research was conducted in the Environmental Protection Area of Conceição da Barra (APA) and the Comboios Biological Reserve (RBC) located in the state of Espírito Santo, Brazil, south-eastern Brazil. Five independent biological replicates of *A. arenaria* and *G. pernambucensis* were selected at each site for nutritional and chlorophyll *a* fluorescence analysis. Soil samples from APA and RBC had similar metal concentrations and physical properties. Five years after the dam rupture, *A. arenaria* had absorbed As, Pb, and V. The increased amounts of heavy metals absorbed did not significantly impair the OJIP curve configuration in both species during the evaluated periods. However, *A. arenaria* at RBC during the rainy season showed increases in the values of φR_0, φP_0, PI_{TOTAL}, and φE_0. Cluster analysis indicated that ChlF in both species was more sensitive to variations in heavy metals within plant tissues. Then, ChlF variation indicated that *A. arenaria* and *G. pernambucensis* exhibited an acclimation strategy in response to increased absorption of heavy metals.

Keywords: Heavy metal; Photosynthesis; Woody plants; Environmental impact; JIP test;

Abbreviations:

ABS: absorbance,
Chl: chlorophyll
CS: cross-section
DI: dissipation
ET: electron transport
Fm: maximum fluorescence level
F_0: minimal fluorescence level
$\varphi P_0 = TR_0/ABS = F_v/F_m$: maximum quantum yield of primary photochemical reactions (at t = 0) that indicates the probability of trapping the energy of absorbed photons (or excitons migrating over the antenna) by PSII reaction centers.
$\varphi E_0 = ET_0/ABS$ = quantum efficiency of electron transfer from Q_A^- to electron transport chain beyond Q_A^-
φR_0 = quantum yield for the reduction of terminal electron acceptors on the acceptor side of PSI .
$ABS/RC = \varphi R_0 = RE/ABS$: proportion between the amounts of chlorophyll *a* molecules in fluorescence-emitting antenna complexes and in the active reaction centers.

TR_0/RC: flux of excitation energy trapped per active reaction center (RC) at the start of illumination of a dark-adapted sample, i.e., at t = 0.
DI_0/RC: total energy dissipated per reaction center (RC) as heat, fluorescence, and energy transfer to PSI (at t = 0).
ET_0/RC: electron flux transferred per active reaction center (RC) at t = 0.
RE_0/RC: electron flux transferred per active reaction center (RC) and reducing terminal acceptors on the acceptor side of PSI (at t = 0).
ΔWOI: serves to distinguish the sequence of events from exciton trapping by PS II up to plastoquinone (PQ) reduction.
ΔWOJ: reveals information about the oxygen-evolving complex functionality (OEC).
ΔWJI: provides information about the reduction of the intersystem electron carriers Q_B, PQ, and Cyt b_6/f, which was defined by their size, mainly of PQ, and the rate constants of the reactions.
Vt = variable fluorescence.
PEA: Plant Efficiency Analyser.
PI: performance index on absorption basis.
OEC: oxygen-evolving complex functionality.
PQ: plastoquinone
PSII: photosystem II
Q_A: primary electron acceptor of PSII
RC: reaction center
TR: trapping

Introduction

Allagoptera arenaria (Gomes) Kuntze (Arecaceae) and *Guapira pernambucensis* (Casar.) Lundell (Nyctaginacea) are species commonly found in “restinga” ecosystems, broadly distributed across fragments of the Atlantic Rainforest that has important ecological functions. *A. arenaria,* commonly known as "guriri," is a palm species that reaches a height of about 2 meters. It forms dense populations that modify the environment under their canopy through litter accumulation, increased soil nutrient content, shade, and decreased wind speed. These modifications facilitate the establishment of other plant species underneath its canopy (Scarano 2002; Menezes et al. 2018). Furthermore, *A. arenaria* is a pioneer species that provides better conditions for the establishment of *G. pernambucensis*, commonly known as "maria-mole" and "joão-mole". *G. pernambucensis* has purple fleshy fruits that attract animal dispersers, promoting seedling recruitment under their canopy and facilitating the regeneration of other species (Dalotto et al. 2018; Flora do Brasil 2022).

The restinga is denomination as a Quaternary sandy coastal plain ecosystem that is part of the Atlantic Forest located along the Eastern Brazilian coast (Brito et al. 2018; Bechara et al. 2020). Restingas soil is composed of sediments classified as marine quartz sands and is naturally nutrient-poor (Monteiro et al. 2014; Bechara et al. 2020). Soil attributes combined with water availability, organic matter content, and salinity determine the variation in restinga plant communities (Bona et al. 2020; Lourenço Júnior et al. 2021). In heterogeneous environments, the physiological responses of plants depend on the simultaneous action of multiple stresses by seasonal variations in climate (Pandey et al. 2015). Research on the physiological responses of plants to environmental resource gradients is important for the prediction of ecosystem responses to environmental changes (Ghori et al. 2019; Souri et al. 2019; Lana-Costa et al. 2021; Tognella et al. 2022; Oliveira et al. 2022).

Restingas are exposed to progressive increases in concentrations of metals from industrial, mining and agricultural activities (Silva et al. 2015; Silva et al. 2017; Lana-Costa et al. 2021; Oliveira et al. 2022). In November 2015, approximately, 50 million m^3 of mud containing heavy metals (Pb, As, Sr, Zn, Cu, Ni and Co) polluted the Doce River, after the collapse of the Fundão Dam in Minas Gerais, Brazil (Marta-Almeida et al. 2016; Cruz et al. 2020; Viana et al. 2020; Sá et al. 2021). As a result, there was a shift in the granulometric fraction of the sediment and an elevation in heavy metal concentrations (Viana et al. 2020). The Fe, Cd, and Mg levels in the post-disaster ore tailing sediments were markedly above the reference values recommended by the National Environment Council, CONAMA (Duarte et al. 2021; Fernandes et al. 2022). The contaminated particles spread for hundreds of kilometres throughout the coastal regions, where the main sources of nutrients are from salt spray deposition and flooding (Du and Hesp 2020). The mobility, bioavailability, and toxicity of heavy metals in the soil are driven by several physio-chemical gradients, such as pH, organic matter, cation exchange capacity, texture, and microbiota (Santos-Filho et al. 2013; Khan et al. 2015).

The available metals in soil may be incorporated into the local food chain, causing ecosystem imbalances (Dubey et al. 2018; Nivelais et al. 2023). An increase in the absorption of heavy metals by plants may cause changes in the mineral nutrient uptake and damage intermediate photosystem electron transporters (Silva et al. 2015; Hanelt 2018). Thus, transient chlorophyll *a* fluorescence (ChlF) is a useful tool for understanding the photochemical effects, through the construction of OJIP curves and the analysis of JIP test parameters (Stirbet et al. 2018). The OJIP curve is derived from the temporal changes in fluorescence intensity (F) following the application of a brief light pulse to a photosynthetic sample, and corresponds to the gradual reduction of Q_A and primary electron acceptor of photosystem II (PSII) (Tsimilli-Michael 2020). The curve derives its name from the distinct steps it exhibits, namely O, J, I, and P Step O corresponds to the initial fluorescence level (F_0) observed prior to the onset of the light pulse and step J is characterized by the peak fluorescence rise (F_J), which represents the reduction of the primary electron acceptor, $Q_A^{-\cdot}$(Goltsev et al. 2016). The O–J phase of the fluorescence rise relates to the closure of some of the PSII reaction centers in response to the reduction of Q_A to a level determined by the ratio between the trapping rate and Q_A reoxidation rate by Q_B and the rest of the electron transfer chain (Kalaji et al. 2016). The J–I phase of the curve corresponds to the reduction of the secondary electron acceptor Q_B, plastoquinone (PQ), cytochrome (Cyt b_6f), and plastocyanin (PC). Finally, I-P phase reflects the reduction of electron transporters (ferredoxin, intermediary acceptors, and NADP) of the PSI acceptor side (Tsimilli-Michael 2020). Analysis of OJIP transients allows researchers to better understand relationships between the structure and function of the photosynthetic apparatus and quickly assess plant viability (Goltsev et al. 2016). The performance of PSII depends on the rate of NADPH consumption during the carbon reactions of photosynthesis, as well as the rate at which the entire plant utilizes assimilates (Kalaji et al 2016). The increased absorption of heavy metals by plants can be correlated with PSII activity (Ghori et al. 2019). For example, iron (Fe) toxicity caused a decrease in PSII activity, an increase in the antenna complex size, and a decrease in the number of active reaction centres in PSII when *Hordeum vulgare* was studied (Lysenko et al. 2020). Previous studies have shown the harmful effects of heavy metals on growth and development of restinga species that exhibited different physiological responses depending on levels of intraspecific tolerance (Silva et al. 2015; Silva et al. 2017; Cruz et al. 2020). Certain species can be very efficient in the accumulation and tolerance of heavy metals, such as *Pteris vittata*, *Isatis cappadocica*, and *Vigna unguiculata* (Ghori et al. 2019; Souri et al. 2019). *I. cappadocica* employs a primary tolerance strategy to excess arsenic (As) by elevating thiol levels, such as through the synthesis of cysteine, glutathione, or phytochelatins (Souri et al. 2019). Another tolerance mechanism is enclosed in a separate compartment and removing heavy metal from the cytosol away from other cellular organelles (Ghori et al. 2019). Investigation of the native restinga species with potential for high tolerance to the heavy metal is essential to understand these mechanisms (Lana-Costa et al. 2021; Oliveira et al. 2022). Thus, ChlF can be effectively used to predict the magnitude of the impacts of absorbed metals on the coastal restinga vegetation subjected to different rainfall regimes. This research aimed to test the hypothesis that changes in precipitation regimes and soil properties could have a significant impact on the absorption of heavy metals by *A. arenaria* and *G. pernambucencis*, leading to changes in (ChlF). Furthermore, a detailed post-disaster analysis was carried out over time using photochemical efficiency indicators to determine the impact of the metals present in mining tailings on these two restinga shrub species.

Materials and methods

Study area and Experimental design

The study was undertaken on the vegetation of an open-scrub bush restinga formation located in the state of Espírito Santo, Brazil, which had been affected by tailings released into the Doce River over the last 4 years following the collapse of the Fundão dam. Two sites were selected based on their location in relation to the mouth of the Doce River where toxic waste entered the water following the rupture of the Fundão Dam in 2015 near to the city of Mariana, Brazil. The Environmental Protection Area of Conceição da Barra (APA) (18°36'26" S, 39°44'50" W) is located approximately 125 km north of the mouth of the Doce River. APA is a conservation area which allows human occupation and exploitation of its natural resources. The Biological Reserve of Comboios (RBC) (19°40'16.50"S, 39°52'57.59"W) is located approximately 5km south of the mouth of the Doce River. RBC is a conservation unit which prohibits any human activity. At each sample site, five individual *Allagoptera arenaria* and *Guapira pernambucensis* plants were selected and marked, according to their health and size homogeneities. The selection of these species was based on their ecological significance and prevalence within the examined restinga ecosystems.

The climate of this area is classified as Aw (Tropical wet-dry), with two distinct dry and rainy seasons. The dry season spans from November to April, while the rainy season lasts from May to October (SANTOS et al. 2018). For this study, meteorological data were obtained from Brazil's National Institute of Meteorology (INMET). The average monthly rainfall in this location varies between 0 and 350 mm, with the majority of precipitation occurring between November and January. Conversely, precipitation deficits occur from June to August. The precipitation means for February 2019, January 2020, and June 2021 were 88 mm, 227 mm, and 0 mm, respectively (Supplementary material; Fig. S1). Leaf and soil samples were collected for analysis of heavy metal concentration, and ChlF was measured under field conditions in February 2019 (reference), January 2020 (rainy season), and June 2021 (dry season).

Chlorophyll *a* fluorescence

During the experimental period (2019, 2020 and 2021), measurements of chlorophyll *a* fluorescence (ChlF) were conducted using four leaves from five plants of each species. Initially, leaves were dark-adapted with leaf clips for 1 h, and then ChlF was measured between 8 am and 10 am, using a portable fluorometer (HandyPEA, Hansatech Instruments®, King's Lynn, Norfolk, UK). The fluorescence transient was induced by red light of approximately 3000 μmol photons m^{-2} s^{-1}, provided by an array of 3 light-emitting diodes with a peak of 660 nm. The fluorometer data was obtained between 20 μs and 1 s of illumination (Strasser et al 2000; 2004). For the construction of the OJIP curve, the following fluorescence intensity values from the original measurements were used: minimal intensity at 20 μs (O step = F_0, initial fluorescence); intensity at 2 ms (the J step); intensity at 30 ms (the I step); and the maximal intensity at 300 ms (the P step = F_m, maximum fluorescence). The different steps of the polyphasic fluorescence transient (O, J, I, and P phases) were calculated to assess possible specific differences in the shapes of the ChlF transients. To evaluate the samples, events represented by the O-J, O-I, and I-P phases, the transients were transformed into relative variable fluorescence (W), according to Yusuf et al. (2010). This involved normalizing the transients using the following equations: $\Delta WOJ = (F_t - F_0) / (F_J - F_0)$, $\Delta WOI = (F_t - F_0) / (F_I - F_0)$, and $\Delta WJI = (F_J - F_I) / (F_I - F_0)$. In addition, we also calculated differential kinetics, ΔW=W−W reference (“reference” were samples collected from APA and RBC in February 2019).

The biophysical parameters derived from the OJIP transients were calculated, and the following parameters, which refer to time zero, i.e., onset of fluorescence induction, were used to calculate maximum quantum yield of PSII photochemistry (φP_0), quantum efficiency of electron transfer from Q_A^- to electron transport chain beyond Q_A^- (at t = 0) (ψE_0), indicating the integral functional activity of PSII, PSI, and the intersystem electron transport chain, and the performance indexes (PI_{TOTAL}, PI_{ABS}), an indicator of impact of a stress on photosynthetic performance (Goltsev et al. 2016). Some JIP parameters, which refer to a translation of the original data into the following biophysical parameters that quantify the PSII behavior, were also evaluated: absorption energy flux per active reaction center (RC); reflecting the proportion between the amounts of chlorophyll molecules in fluorescence-emitting antenna complexes and in the active reaction centers (ABS/RC), flux of excitation energy trapped per active reaction center (RC) at the start of illumination of a dark-adapted sample, i.e., at t = 0 (TR_0/RC), —total energy dissipated per reaction center (RC) as heat, fluorescence, and energy transfer to PSI (at t = 0) (DI_0/RC), electron flux transferred per active reaction center (RC) at t = 0 (ET_0/RC), electron flux transferred per active reaction center (RC), and reducing terminal acceptors on the acceptor side of PSI (at t = 0) (RE_0/RC) (Goltsev et al. 2016; Tsimilli-Michael 2020). In our study, data from February 2019 were used as the reference because there are no records available of normal concentrations of heavy metals before the collapse of the Fundão Dam.

Heavy metal levels and soil fertility analyses

Samples of mature, healthy, sun-exposed leaves from five individuals of each plant species, as well as soil samples, were collected during the experimental period (2019, 2020, and 2021) for micronutrient analysis. At each sample site, leaf samples were taken from each individual and combined to create a composite sample for plant heavy metal analyses, which were conducted in triplicate. Soil samples were obtained from the root zone of each tree at a depth of 0.20 m using a soil auger and then stored in plastic bags. Both the soil and leaf samples were dried in a forced circulation oven at 70°C for 72 hours. After drying, the samples were homogenized and subjected to extraction using an acid solution. The nutrients present in the soil and leaf samples were quantified using optical emission spectrometry with inductively coupled plasma (ICP-OES), following the method described by Huang and Schulte (1985).

In addition to the micronutrient analysis, the following soil fertility analyses were performed according to the Brazilian Methods of Soil Analysis (Santos et al. 2018): soil pH, cation exchange capacity (T), exchangeable aluminum content (Al^{3+}), potential soil acidity (H+Al), sum of the bases (SB), base saturation result (V%) and soil organic matter (OM). The extraction of exchangeable potassium (K), phosphorus (P), and boron (B) in the soil was conducted using the Mehlich-1 solution. Furthermore, the granulometric analysis of the soil involved passing the soil samples through a 2 mm sieve to measure the size distribution of individual soil particles.

Statistical analysis

A. arenaria and *G. pernambucencis* were selected at each site under field conditions. Five independent biological replicates were used to assess the variability in the results for chlorophyll *a* fluorescence, mineral element levels, and soil fertility analyses. Data were submitted to analysis of variance (ANOVA) and the statistical difference between means were compared using the Tukey test ($P < 0.05$). In order to categorize the treatments based on their measured traits, a cluster analysis method was employed. Before the analysis, all the data was standardized. Ward's method and Euclidean distance were utilized to group the treatments. A dendrogram was produced, and a line was marked at the cutoff point which aided in identifying the clusters. Treatments that shared similar features were grouped together into one cluster.

Results

Soil analysis

The fertility results were compared to Espírito Santo State soil reference values, according to the classification proposed by Prezotti and Guarçoni (2013). All of the sites were considered to have medium acidity (pH = 5.1 - 5.9), except for RBC during the rainy season, which showed reduced acidity (pH > 6.0). The exchangeable aluminum content (Al^{3+}) was considered low (< 0.3 $cmol_c\ dm^{-3}$) for all the sites, indicating the absence of aluminum toxicity (Table 1). The effective cation exchange capacity (T), sum of the bases (SB) and organic matter content (OM) were considered low (< 25 $mmol_c\ dm^{-3}$, < 2 $mmol_c\ dm^{-3}$ and <1.5 dag kg^{-1}, respectively) for all of the sites. All of the sites had reduced P contents (< 20 mg kg^{-1}), Ca^{2+} (< 1.5 mmol$_c$ dm^{-3}), Mg^{2+}(< 5 mmol$_c$ dm^{-3}) and B (< 0.35 mg kg^{-1}). The base saturation (V%) was considered average (50 to 70%) for RBC during the reference period and low (< 50%) for RBC during the rainy and dry seasons (Table 1).

Table 1 Physical and chemical soil properties (layer: 0–20 cm) of the Environmental Protection Area of Conceição da Barra (APA) and the Comboios Biological Reserve (RBC) during the rainy and dry seasons

	Reference		Rainy		Dry	
	APA	RBC	APA	RBC	APA	RBC
pH ($CaCl_2$)	5.4 ± 0.1 b	5.4 ± 0.0 b	5.4 ± 0.1 b	6.1 ± 0.1 a	5.7 ± 0.1 b	5.6 ± 0.1 b
Al^{3+}(cmol$_c$ dm^{-3})	0.1 ± 0.1 a	0.0 ± 0.0 a	0.0 ± 0.0 a	0.0 ± 0.0 a	0.0 ± 0.0 a	0.0 ± 0.0 a
H+Al (cmol$_c$ dm^{-3})	1.9 ± 0.2 a	0.4 ± 0.1 b	0.7 ± 0.1 b	0.3 ± 0.0 b	0.6 ± 0.0 b	0.3 ± 0.0 b
SB (cmol$_c$ dm^{-3})	1.5 ± 0.1 a	0.7 ± 0.2 a	0.3 ± 0.0 b	0.2 ± 0.0 b	0.3 ± 0.0 b	0.3 ± 0.0 b
T (cmol dm^{-3})	3.4 ± 0.1 a	1.1 ± 0.2 b	1.0 ± 0.1 bc	0.5 ± 0.0 d	0.8 ± 0.0 bcd	0.6 ± 0.0 cd
V (%)	44.2 ± 3.3 b	63.8 ± 1.9 a	31.1 ± 2.4 b	43.7 ± 2.5 b	32.5 ± 3.0 b	44.5 ± 5.2 b
OM (dag Kg^{-1})	1.9 ± 0.1 a	0.5 ± 0.2 b	0.3 ± 0.0 bc	0.1 ± 0.0 c	0.2 ± 0.0 bc	0.2 ± 0.0 bc
P (mg kg^{-1})	2.0 ± 0.2 ab	2.6 ± 0.9 a	1.3 ± 0.1 ab	0.7 ± 0.1 b	1.0 ± 0.1 ab	1.2 ± 0.2 ab
S (mg kg^{-1})	6.8 ± 0.2 a	6.9 ± 0.2 a	5.1 ± 0.4 b	3.2 ± 0.2 c	2.8 ± 0.2 c	3.0 ± 0.3 c
B (mg kg^{-1})	0.2 ± 0.0 a	0.1 ± 0.0 b	0.2 ± 0.0 a	0.2 ± 0.0 a	0.2 ± 0.0 ab	0.1 ± 0.0 ab
K (mg kg^{-1})	24.0 ± 4.0 a	13.5 ± 4.9 ab	1.3 ± 1.3 bc	4.0 ± 1.2 bc	0.0 ± 0.0 c	0.0 ± 0.0 c
Ca^{2+} (cmol$_c$ dm^{-3})	1.0 ± 0.1 a	0.5 ± 0.1 b	0.2 ± 0.0 c	0.1 ± 0.0 c	0.2 ± 0.0 c	0.2 ± 0.0 c
Mg^{2+} (cmol$_c$ dm^{-3})	0.5 ± 0.0 a	0.2 ± 0.1 b	0.1 ± 0.0 b	0.1 ± 0.0 b	0.1 ± 0.0 b	0.1 ± 0.0 a
Coarse sand (%)	0.9 ± 0.0 c	0.9 ± 0.0 c	95.6 ± 0.4 a	96.4 ± 0.2 a	89.6 ± 0.2 b	95.0 ± 0.5 a
Fine sand (%)	0.0 ± 0.0 c	0.0 ± 0.0 c	2.5 ± 0.4 b	2.0 ± 0.2 b	4.6 ± 0.1 a	0.9 ± 0.1 c
Silt (%)	0.0 ± 0.0 c	0.0 ± 0.0 c	0.4 ± 0.3 bc	1.1 ± 0.2 b	2.3 ± 0.2 a	1.0 ± 0.2 b
Clay (%)	0.0 ± 0.0 c	0.0 ± 0.0 c	1.5 ± 0.3 c	0.5 ± 0.2 bc	3.4 ± 0.3 a	3.1 ± 0.3 a

Values are the means of three replicates with standard deviation (± SD). Values followed by the same letter(s) were not significantly different according to the Tukey test at P.≤ 0.5.

Fe, Mn, V, Cr, Pb, and As were the heavy metals with the highest concentrations in APA and RBC during the different periods. The order of metal concentrations in the soil was Fe> Mn> V> Cr> Pb>As> Ni> Zn> Co> Cu> Cd> at APA and RBC over the different periods. All sites had reduced concentrations of Zn and Cu (< 1 mg kg^{-1} and < 0.8 mg kg^{-1}, respectively). APA during the rainy season showed medium availability of Fe (20 – 45 mg kg^{-1}) and the other sites had reduced concentrations of Fe (< 20 mg kg^{-1}). APA during dry season showed reduced availability of Mn (< 5 mg kg^{-1}) and the RBC site had an average Mg concentration of 5 – 12 mg kg^{-1}. In general, heavy metal concentrations in the soil were not affected by the differences in rainfall intensity between rainy and dry seasons (Table 2).

Table 2 Levels of heavy metals in soil at the Environmental Protection Area of Conceição da Barra (APA) and the Comboios Biological Reserve (RBC) during the rainy and dry seasons

	Reference		Rainy		Dry	
	APA	RBC	APA	RBC	APA	RBC
Cu	0.3 ± 0.0 ab (100)	0.3 ± 0.0 a (100)	0.3 ± 0.0 a (100)	0,2 ± 0,0 ab (67)	0,1 ± 0,0 b (33)	0,3 ± 0,1 a (100)
Mn	16.1 ± 1.3 a (100)	17.0 ± 1.6 a (100)	7.5 ± 0.4 bc (47)	11,8 ± 1,3 ab (69)	4,5 ± 0,3 c (28)	8,0 ± 1,9 bc (47)
Fe	22.5 ± 1.8 a (100)	16.5 ± 2.0 ab (100)	12.4 ± 0.8 b (55)	10,8 ± 1,5 b (65)	12,9 ± 0,4 b (57)	11,4 ± 0,2 b (69)
Zn	0.6 ± 0.0 a (100)	0.7 ± 0.1 a (100)	0.3 ± 0.0 c (50)	0,4 ± 0,0 bc (57)	0,1 ± 0,0 c (17)	0,2 ± 0,0 c (29)
Cr	5.6 ± 1.0 ab (100)	9.5 ± 1.1 a (100)	2.4 ± 0.5 b (43)	5,3 ± 2,9 ab (56)	3,8 ± 1,1 ab (68)	3,6 ± 0,2 ab (38)
Co	0.5 ± 0.1 a (100)	1.7 ± 0.1 d (100)	0.6 ± 0.0 d (120)	1,0 ± 0,1 bc (59)	0,8 ± 0,1 cd (160)	1,3 ± 0,1 ab (76)
As	2.3 ± 0.2 b (100)	1.8 ± 0.0 b (100)	2.6 ± 0.2 b (113)	2,5 ± 0,3 b (139)	4,0 ± 0,3 a (174)	4,4 ± 0,3 a (244)
Cd	0 ± 0 b 100)	5.4 ± 3.1 a (100)	0.1 ± 0.0 a (100)	0,1 ± 0,0 a (2)	0,1 ± 0,0 a (100)	0,1 ± 0,0 a (2)
Ni	1.5 ± 0.1 ab (100)	2.5 ± 0.1 a (100)	1.0 ± 0.8 ab (67)	0,2 ± 0,0 ab (8)	0,9 ± 0,1 ab (60)	1,7 ± 0,2 ab (68)
Pb	2.6 ± 0.7 b (100)	5.5 ± 1.1 a (100)	0.9 ± 0.1 b (35)	1,0 ± 0,2 b (18)	1,2 ± 0,1 b (46)	1,0 ± 0,2 b (18)
V	5.9 ± 0.9 ab (100)	7.4 ± 0.4 a (100)	4.0 ± 0.3 b (68)	4,4 ± 0,6 ab (59)	6,2 ± 0,4 ab (105)	5,8 ± 0,4 ab (78)

Values are the means of three replicates with standard deviation (± SD). Values followed by the same letter(s) were not significantly different according to the Tukey test at $P \leq 0.5$. Values in parentheses represent differences between the rainy and dry seasons when compared to the reference period.

Metal concentrations in leaves

The concentrations of essential elements (Cu, Mn, Fe, Zn, Co) and non-essential elements (Cr, Cd, Ni, Pb, V) in *A. arenaria* were similar between the APA and RBC sites during the reference period (February 2019). However, the concentrations of As, Pb and V in *A. arenaria* leaves were higher at RBC during the rainy season than during the reference period (Table 3). The order of leaf-metal concentrations in *A. arenaria* at RBC was Fe > Zn > Cu > Cr > Ni > Pb > V > As > Cd > Co. The concentration of As in *A. arenaria* during the reference period varied between 0.3 mg kg^{-1} (APA) and 0.2 mg kg^{-1} (RBC), whereas during both the rainy and dry periods, the concentration of As was 1.1mg kg^{-1} at both sites. Similarly, Pb concentration in *A. arenaria* during the reference period varied between 0.1 mg kg^{-1} (APA) and 0.2 mg kg^{-1} (RBC), while during both the rainy and dry periods, the concentration was 1.9 mg kg^{-1} at both sites. The V concentration (2.5 mg kg^{-1}) were higher in *A. arenaria* at RBC during the rainy season (Table 3). The concentrations of essential (Cu, Mn, Fe, Zn, Co) and non-essential elements (Cr, Cd, Ni, Pb, V) in *G. pernambucensis* varied among the areas during the same period, with the highest concentrations of Co (4.4 mg kg^{-1}), Cu (70 mg kg^{-1}), Mn (775 mg kg^{-1}), Ni (6.3 mg kg^{-1}), and V (4.3 mg kg^{-1}) at RBC during the rainy season. The order of metal concentrations in *G. pernambucensis* at RBC was Mn> Fe > Cu> Zn > Cr > Ni > Co >V >Pb > As > Cd at RBC during the rainy season (Table 3).

Table 3 Levels of heavy metals in leaves from *Allagoptera arenaria* and *Guapira pernambucencis* during the rainy and dry seasons at the Environmental Protection Area of Conceição da Barra and the Comboios Biological Reserve

		Reference		Rainy		Dry	
		APA	RBC	APA	RBC	APA	RBC
Allagoptera arenaria	Cu	12.7 ± 3.9 a (100)	5.5 ± 2.5 ab (100)	2.0 ± 0.3 b (16)	10.1 ± 0.9 ab (184)	1.7 ± 0.2 b (13)	2.9 ± 0.2 b (53)
	Mn	224.8 ± 7.7 b (100)	513.6 ± 109.8 ab (100)	170.4 ± 19.4 b (76)	276.8 ± 37.0 ab (54)	214.0 ± 10.3 b (95)	697.3 ± 186.6 a (136)
	Fe	109.6 ± 0.0 ab (100)	109.6 ± 0.0 ab (100)	168.4 ± 30.6 a (154)	69.2 ± 4.8 b (63)	162.7 ± 24.3 a (148)	143.7 ± 27.3 ab (131)
	Zn	11.7 ± 1.1 a (100)	18.1 ± 2.1 a (100)	14.4 ± 4.1 a (123)	14.4 ± 1.5 a (80)	7.0 ± 0.4 a (60)	24.1 ± 7.6 a (133
	Cr	0.8 ± 0.2 b (100)	0.6 ± 0.0 b (100)	1.0 ± 0.2 b (125)	8.3 ± 1.8 a (1383)	1.1 ± 0.5 b (138)	0.6 ± 0.0 b (100)
	Co	0.0 ± 0.0 a (100)	0.0 ± 0.0 a (100)	0.0 ± 0.0 a (100)	0.1 ± 0.0 a	0.0 ± 0.0 a	0.2 ± 0.2 a (100)
	As	0.3 ± 0.1 b (100)	0.2 ± 0.0 b (100)	1.1 ± 0.0 a (367)	1.1 ± 0.0 a (550)	1.1 ± 0.0 a (367)	1.1 ± 0.0 b (550)
	Cd	0.0 ± 0.0 a	0.0 ± 0.0 a	0.0 ± 0.0 a	0.0 ± 0.0 a (	0.0 ± 0.0 a	0.1 ± 0.0 a
	Ni	0.1 ± 0.0 b (100)	0.7 ± 0.4 b (100)	1.2 ± 0.6 b (1200)	3.2 ± 0.4 a (457)	0.7 ± 0.0 b (700)	0.6 ± 0.4 b (86)
	Pb	0.1 ± 0.0 b (100)	0.2 ± 0.1 b (100)	1.9 ± 0.0 a (1900)	1.9 ± 0.0 a (950)	1.9 ± 0.0 a (1900)	1.9 ± 0.0 a (950)
	V	0.5 ± 0.2 b (100)	0.1 ± 0.0 b (100)	0.7 ± 0.1 a (140)	2.5 ± 0.5 b (2500)	0.5 ± 0.2 a (100)	0.2 ± 0.0 a (200)
Guapira pernambucensis	Cu	13.5 ± 2.6 b (100)	22.3 ± 3.5 b (100)	10.5 ± 0.7 b (78)	70.0 ± 8.4 b (314)	10.9 ± 0.4 b (81)	6.9 ± 1.2 a (31)
	Mn	181.2 ± 51.6 d (100)	418.7 ± 18.1 bc (100)	228.5 ± 17.9 cd (126)	774.9 ± 72.8 a (185)	292.0 ± 6.5 cd (161)	571.3 ± 55.8 ab (136)
	Fe	168.1 ± 16.5 b(100)	109.6 ± 0.0 b (100)	306.9 ± 15.0 a (183)	114.6 ± 19.3 b (105)	319.3 ± 20.4 a (190)	200.3 ± 38.8 b 183)
	Zn	15.1 ± 1.9 a (100)	23.0 ± 2.9 a (100)	13.4 ± 1.5 a (89)	19.0 ± 2.9 a (83)	14.6 ± 1.1 a (97)	13.8 ± 2.0 a (60)
	Cr	3.2 ± 0.7 b (100)	3.0 ± 0.2 b (100)	2.2 ± 0.2 b (69)	14.2 ± 1.8 a (473)	3.6 ± 0.9 b (113)	4.0 ± 0.6 b (133)
	Co	0.3 ± 0.0 b (100)	0.6 ± 0.1 b (100)	0.3 ± 0.0 b (100)	4.4 ± 1.0 a (733)	0.6 ± 0.0 b (200)	0.6 ± 0.3 b (100)
	As	0.8 ± 0.1 b (100)	0.6 ± 0.1 c (100)	1.1 ± 0.0 a (138)	1.1 ± 0.0 a (183)	1.1 ± 0.0 a (138)	1.1 ± 0.0 a (183)
	Cd	0.0 ± 0.0 a (0)	0.0 ± 0.0 a (0)	0.0 ± 0.0 a (0)	0.0 ± 0.0 a (0)	0.0 ± 0.0 a(0)	0.0 ± 0.0 a
	Ni	0.1 ± 0.0 c (100)	1.3 ± 0.4 b (100)	0.7 ± 0.1 ab (700)	6.3 ± 0.3 a (485)	1.0 ± 0.0 ab (1000)	1.0 ± 0.1 ab (77)
	Pb	0.0 ± 0.0 b (100)	0.1 ± 0.1 b (100)	1.9 ± 0.0 a (100)	1.9 ± 0.0 a (1900)	1.9 ± 0.0 a (100)	1.9 ± 0.0 a (1900)
	V	1.7 ± 0.2 b (100)	0.9 ± 0.0 b (100)	1.1 ± 0.1 b (65)	4.4 ± 0.3 a (489)	1.6 ± 0.3 b (94)	1.4 ± 0.2 b (156)

Values are shown as the means of three replicates with standard deviation (± SD). Values followed by the same letter(s) were not significantly different according to the Tukey test at P ≤ 0.5. Values in parentheses represent differences between rainy and dry seasons when compared to the reference period.

Principal component analysis (PCA) explained 60.3% of the variability in the data (38.6% in PC1 and 21.7% in PC2) and showed a clear separation at the RBC site between the reference, rainy, and dry periods. However, no distinction could be made at the APA site between rainy and dry periods (Fig. 1a). Then, RBC was the most heterogeneous functional group, demonstrating the natural heterogeneity of the biological reserve areas The concentrations of Ni, Cr, Cu, and V in *A. arenaria* at RBC during the rainy season were mainly associated with soil pH (Fig. 1b). RBC during the rainy season also exhibited soil pH mostly associated with the concentrations of Ni, Cr, V, Cu, and Mn in *G. pernambucensis* (Fig. 1b).

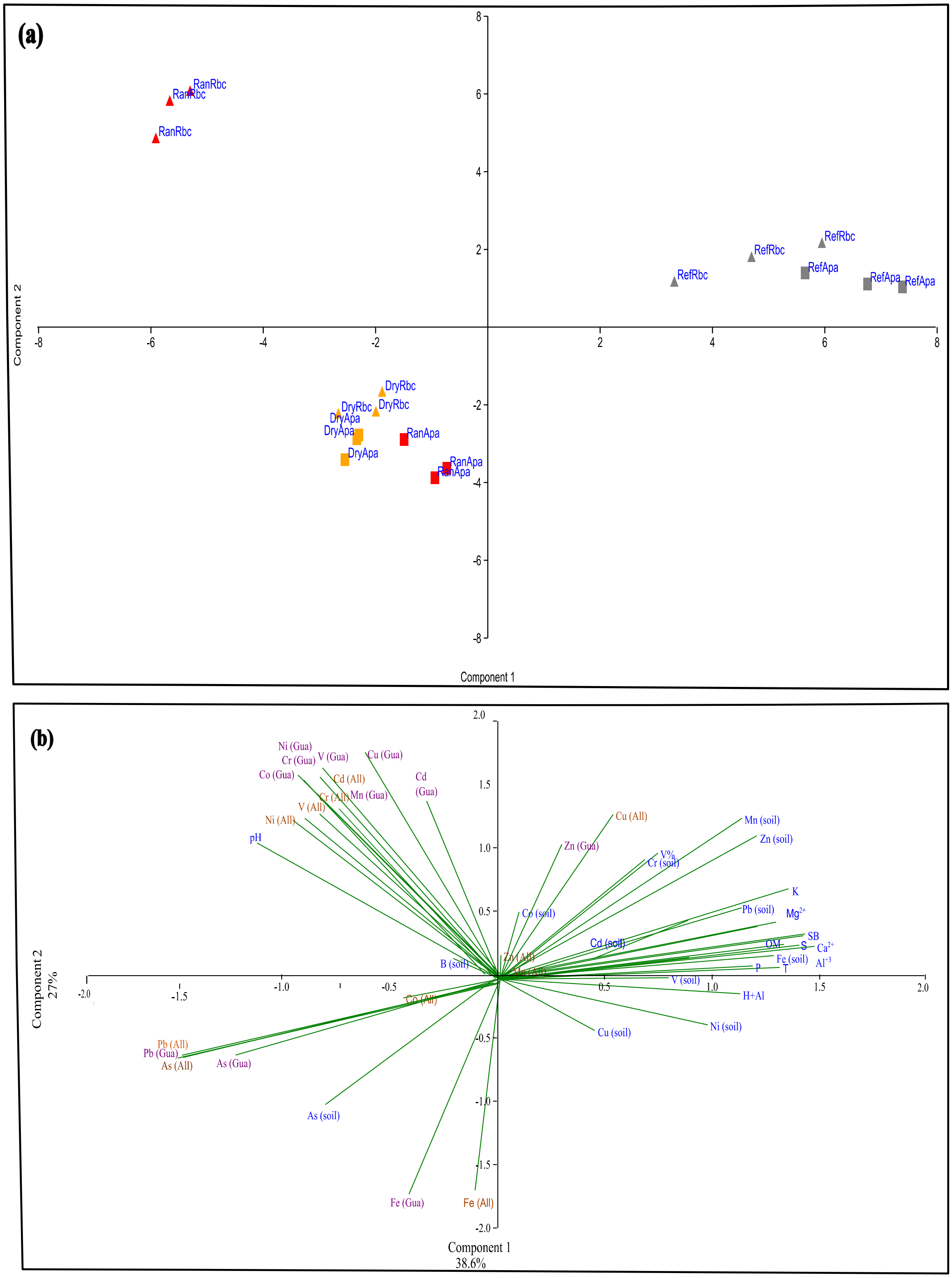

Fig.1 Principal component analysis (PCA) for the relationships between the physical-chemical soil characterization and the heavy metals in *A. arenaria* and *G. pernambucencis* leaves during the rainy and dry seasons at the Environmental Protection Area of Conceição da Barra (APA) and the Comboios Biological Reserve (RBC).

Among the metals associated with the physical-chemical characteristics of the soil, *A. arenaria* and *G. pernambucensis* showed a high ratio between the Mn and Cr concentrations in the soil and the metal concentrations in leaves at RBC during the rainy season (Table 4 and Table 5). The ratio between the metal concentrations in the soil and the metal concentrations in *A. arenaria* leaves was similar at both sites during the reference period (Table 4). The ratio between metal concentrations in the soil and Cu, Mn, Cr, Cd, Ni and V concentrations in leaves were 52.3, 23.5, 1.6, 3.9, 19.0 and 0.6, respectively, for *A. arenaria* at RBC during the rainy season (Table 4). For *G. pernambucencis* at RBC during the rainy season, the ratios of Cu, Mn, Cr, Cd, Ni and V were 362, 65.9, 2.68, 0.54, 37.2 and 1.0, respectively (Table 5). Cu, Mn, and Zn had the highest ratios in *A. arenaria* and *G. pernambucencis*, despite the reduced concentrations in the soil (Table 4 and Table 5).

Table 4 Ratio between metal concentrations in soil (mg kg^{-1}) and leaves (mg kg^{-1}) of *A. arenaria* at Environmental Protection Area of Conceição da Barra (APA) and the Comboios Biological Reserve (RBC) during the rainy and dry seasons

	Reference		Rainy		Dry	
	APA	RBC	APA	RBC	APA	RBC
Cu	49.0 ± 14.5 [ab] (100)	20.8 ± 9.6 [abc] (100)	6.2 ± 1.1 [c] (13)	52.3 ± 7.1 [a] (251)	12.6 ± 0.9 [bc] (26)	10.0 ± 1.9 [c] (48)
Zn	14.0 ± 1.5 [a] (100)	30.3 ± 3.7 [a] (100)	22.6 ± 3.3 [a] (162)	23.5 ± 1.1 [a] (78)	47.2 ± 4.9 [a] (338)	87.5 ± 65.5 [a] (289)
Fe	4.9 ± 0.4 [a] (100)	6.6 ± 0.8 [a] (100)	13.6 ± 2.9 [a] (280)	6.4 ± 1.0 [a] (97)	12.6 ± 2.1 [a] (259)	12.6 ± 2.5 [a] (190)
Zn	18.5 ± 1.4 [b] (100)	24.3 ± 1.1 [ab] (100)	48.5 ± 19.5 [ab] (263)	35.2 ± 1.8 [ab] (145)	53.9 ± 14.2 [ab] (292)	109.5 ± 38.4 [a] (450)
Cr	0.1 ± 0.1 [a] (100)	0.1 ± 0.0 [a] (100)	0.4 ± 0.0 [a] (287)	1.6 ± 0.0 [a] (2617)	0.3 ± 0.0 [a] (200)	0.2 ± 0.0 [a] (283)
Co	0.0 ± 0.0 [a] (0)	0.0 ± 0.0 [a] (0)	0.0 ± 0.0 [a] (0)	0.1 ± 0.5 [a]	0.0 ± 0.1 [a] (0)	0.2 ± 0.4 [a] (100)
As	0.1 ± 0.1 [d] (100)	0.1 ± 0.0 [d] (100)	0.4 ± 0.1 [ab] (1900)	0.4 ± 1.5 [ab] (950)	0.3 ± 0.1 [bc] (1900)	0.2 ± 0.0 [cd] (240)
Cd	0.0 ± 0.0 [b] (0)	0.0 ± 0.0 [b] (0)	0.1 ± 0.0 [b] (0)	3.9 ± 0.0 [a] (100)	0.3 ± 0.0 [b] (100)	0.8 ± 0.2 [b] (100)
Ni	0.1 ± 0.0 [b] (100)	0.3 ± 0.1 [b] (100)	1.2 ± 4.1 [a] (1967)	19.0 ± 2.4 [b] (7037)	0.7 ± 0.1 [b] (1200)	0.4 ± 0.3 [b] (133)
Pb	0.0 ± 0.0 [b] (0)	0.0 ± 0.0 [b] (0)	2.1 ± 0.2 [a] (100)	1.8 ± 0.4 [a] (100)	1.6 ± 0.2 [a] (100)	1.9 ± 0.4 [a] (100)
V	0.1 ± 0.1 [b] (100)	0.0 ± 0.0 [b] (100)	0.2 ± 0.0 [b] (76)	0.6 ± 0.2 [a] (168)	0.1 ± 0.0 [b] (38)	0.0 ± 0.0 [b] (0)

Values are the means of three replicates with standard deviation (± SD). Values followed by the same letter(s) were not significantly different according to of the Tukey test at P ≤ 0.5. Values in parentheses represent differences between the rainy and dry seasons when compared to the reference period.

Table 5 Ratio between metal concentrations in soil (mg kg^{-1}) and leaves (mg kg^{-1}) of *G. pernambucencis* at Environmental Protection Area of Conceição da Barra (APA) and the Comboios Biological Reserve (RBC) during the rainy and dry seasons

	Reference		Rainy		Dry	
	APA	RBC	APA	RBC	APA	RBC
Cu	51.9 ± 13.5^{b} (100)	84.2 ± 14.2^{b} (100)	31.7 ± 1.8^{b} 64	362.1 ± 42.8^{a}	80.1 ± 4.3^{b} (430)	23.9 ± 1.9^{b} (28)
Mn	11.3 ± 2.7^{c} (100)	24.7 ± 2.7^{bc} (100)	30.3 ± 3.4^{bc} (270)	65.9 ± 12.5^{ab} (267)	64.4 ± 2.9^{ab} (573)	71.7 ± 22.1^{a} (290)
Fe	7.5 ± 0.1^{bc} (100)	6.6 ± 0.8^{c} (100)	24.8 ± 0.3^{a} (332)	10.6 ± 3.6^{bc} (160)	24.8 ± 2.1^{a} (331)	17.6 ± 3.3^{ab} (265)
Zn	23.8 ± 2.4^{b} (100)	30.9 ± 8.0^{b} (100)	45.3 ± 4.4^{b} (190)	46.3 ± 6.5^{b} (150)	112.1 ± 25.8^{a} (471)	62.9 ± 11.9^{ab} (204)
Cr	0.6 ± 0.0^{b} (100)	0.3 ± 0.0^{b} (100)	0.9 ± 0.0^{b} (163)	2.7 ± 0.0^{a} (838)	0.9 ± 0.0^{b} (168)	1.1 ± 0.0^{b} (347)
Co	0.5 ± 0.0^{b} (100)	0.3 ± 0.0^{b} (100)	0.5 ± 0.0^{b} (89)	4.4 ± 0.1^{a} (1372)	0.7 ± 0.0^{b} (128)	0.4 ± 0.1^{b} (131)
As	0.4 ± 0.1^{ab} (100)	0.3 ± 0.0^{ab} (100)	0.4 ± 0.2^{ab} (114)	0.4 ± 1.3^{ab} (132)	0.3 ± 0.5^{ab} (72)	0.2 ± 0.1^{b} (77)
Cd	0.0 ± 0.2^{b} (0)	0.0 ± 0.0^{b} (0)	0.1 ± 0.1^{b} (100)	0.5 ± 1.0^{a} (100)	0.1 ± 0.1^{b} (100)	0.2 ± 0.2^{b} (100)
Ni	0.1 ± 0.0^{b} (100)	0.5 ± 0.2^{b} (100)	0.7 ± 1.1^{b} (1133)	37.2 ± 1.7^{a} (6896)	1.1 ± 0.2^{b} (1850)	0.6 ± 0.2^{b} (107)
Pb	0.0 ± 0.0^{b} (0)	0.0 ± 0.0^{b} (0)	2.1 ± 0.2^{a} (100)	1.8 ± 0.4^{a} (100)	1.6 ± 0.2^{a} (100)	1.9 ± 0.4^{a} (100)
V	0.3 ± 0.0^{b} (100)	0.1 ± 0.0^{b} (100)	0.3 ± 0.0^{b} (100)	1.0 ± 0.1^{a} (825)	0.3 ± 0.1^{b} (100)	0.2 ± 0.0^{b} (200)

Values are the means of three replicates with standard deviation (± SD). Values followed by the same letter(s) were not significantly different according to the Tukey test at $P \leq 0.5$. Values in parentheses represent differences between the rainy and dry seasons when compared to the reference period.

The fluorescence rise kinetics

The fluorescence rise OJIP curves for *A. arenaria* and *G. pernambucencis* at RBC and APA were measured to investigate the photochemical efficiency under heavy metal during rainy and dry seasons. *A. arenaria* and *G. pernambucencis* showed typical fluorescence transient curve shapes for all samples (Fig. 2a, b). In *A. arenaria* and *G. pernambucencis,* the fluorescence yield of the OJIP curve at both sites during the rainy and dry seasons was reduced when compared with the reference season. To obtain more detailed information than that provided by raw fluorescence kinetics, the curves were plotted as relative variable fluorescence, $Vt=(Ft–F_0)/ (F_m–F_0)$. The J step for *A. arenaria* at APA was lower during the rainy (24%) and dry (41%) seasons than the reference season. Similarly, the J step for *G. pernambucencis* at RBC was reduced during the rainy (16%) and dry (26%) seasons when compared to the reference season. The magnitude of the J-step measures the availability of oxidized PQ molecules to reoxidize Q_A. Both species at APA and RBC showed similar I-P phases when comparing reference, rainy and dry seasons (Fig. 2c, d).

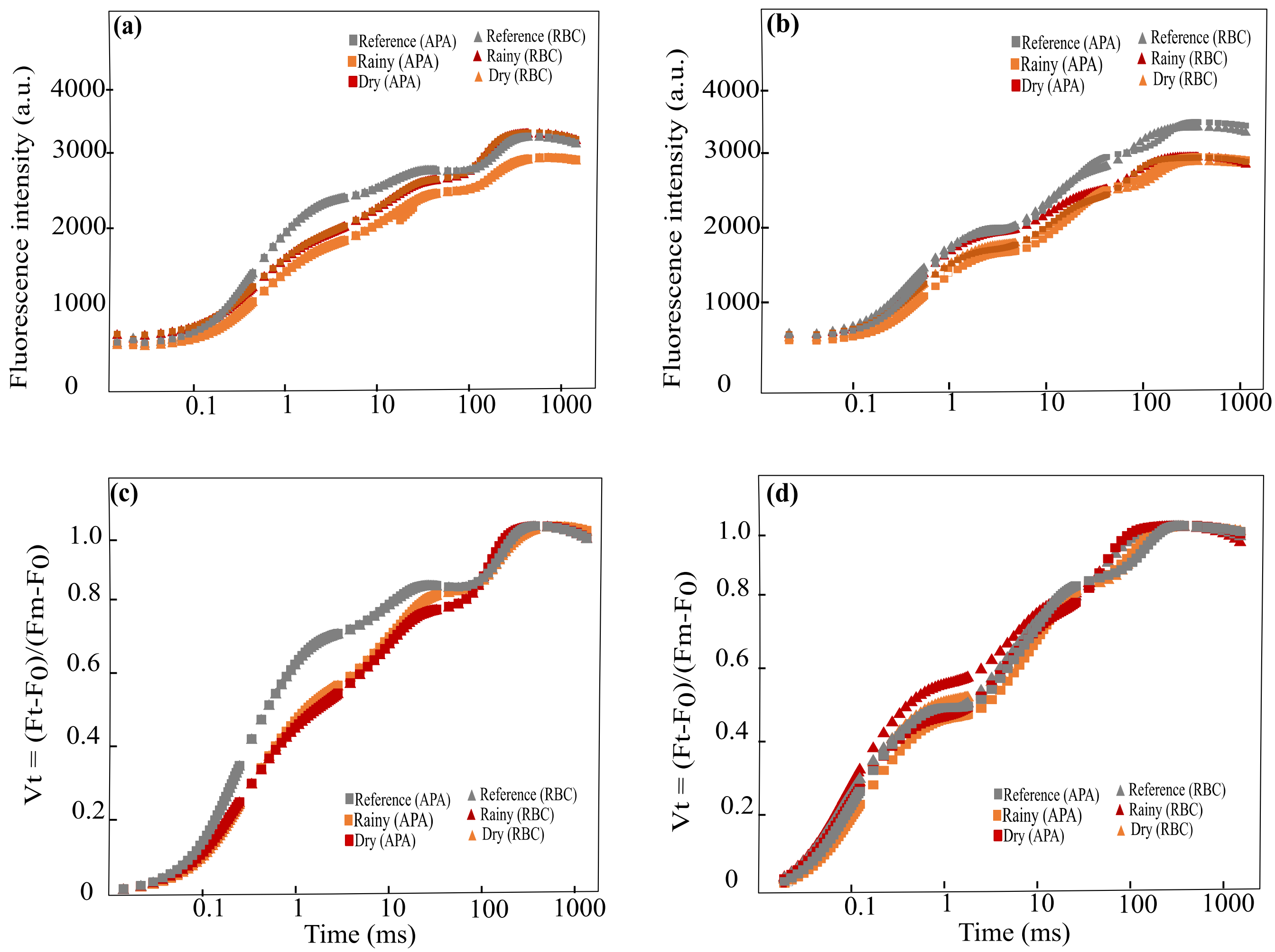

Fig.2 Variations in the shape of fluorescence transient curves measured at different times (rainy and dry seasons) in the leaves of *A. arenaria* and *G. pernambucencis* at the Environmental Protection Area of Conceição da Barra (APA) and the Biological Reserve of Comboios (RBC). Fluorescence intensity of *A. arenaria* (**a**) and *G. pernambucencis* (**b**). Variable fluorescence of *A. arenaria* (**c**) and *G. pernambucencis* (**d**). The reference period corresponds to samples collected from APA and RBC in February 2019.

Detailed examination of the shape of the prompt ChlF curves was conducted by constructing differential curves in the phase between the O and I points (ΔWOI). All *A. arenaria* and *G. pernambucencis* samples were not strongly affected, as indicated by ΔWOI values that approximated 0 (Fig. 3a, b). The differential curves for the phase between the O and J points (ΔWOJ) in both species were not strongly affected as seen from the resulting differential curves with values close to 0 for all samples (Fig. 3c, d). However, reproducible positive bands in the differential curves constructed in the phase between the J and I points (ΔWJI) were found for *A. arenaria* and *G. pernambucencis* at RBC during the rainy season (Fig. 3e, f).

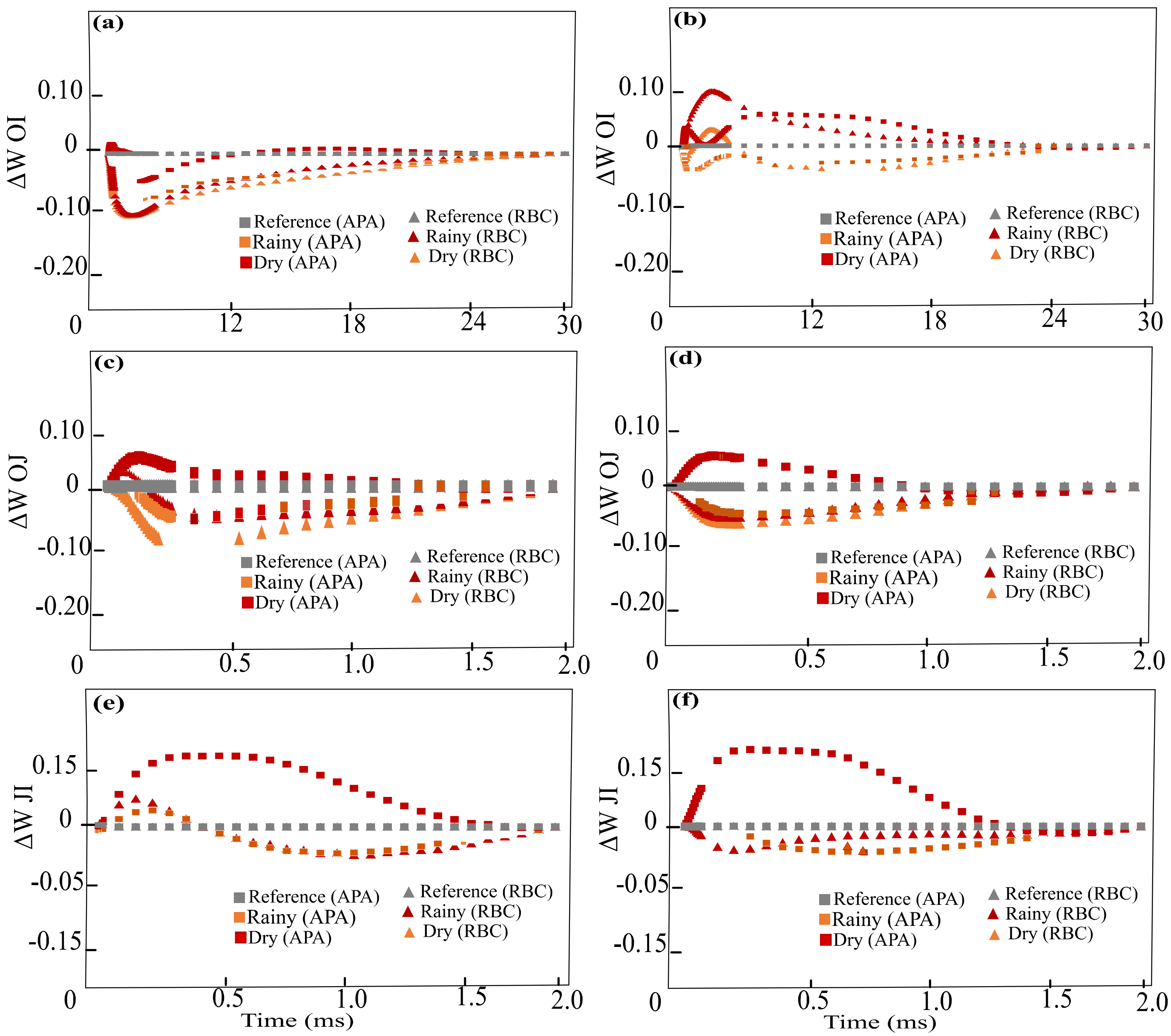

Fig. 3 Relative variable fluorescence (ΔW) [Wseason – Wreference] derived from the average OJIP transient of *A. arenaria* and *G. pernambucencis* at the Environmental Protection Area of Conceição da Barra (APA) and the Comboios Biological Reserve (RBC). Differential curves constructed between the O-I phases $\Delta WOI = (F_t - F_0) / (F_I - F_0)$] for *A. arenaria* (**a**) and *G. pernambucencis* (**b**). Differential curves constructed between the O-J phases [$\Delta WOJ = (F_t - F_0) / (F_J - F_0)$] of *A. arenaria* (**c**) and *G. pernambucencis* (**d**). Differential curves constructed between the J-I phases [$\Delta WJI = (F_J - F_I) / (F_I – F_0)$] of *A. arenaria* (**e**) and *G. pernambucencis* (**f**). The reference period corresponded to samples collected from APA and RBC in February 2019.

For *A. arenaria*, the energy fluxes expressed per active RC as ABS/RC, TR_0/RC and DI_0/RC remained unaffected at RBC during the rainy and dry periods relative to the reference (Fig. 4a). However, the quantum efficiency of electron transfer from Q_A^- to the electron transport chain beyond Q_A^- (φE_0) and quantum yield for the reduction of terminal electron acceptors on the acceptor side of PSI (φR_0) increased by 40% and 36%, respectively, for *A. arenaria* at APA and RBC during the rainy season compared to the reference season. When compared to the reference period, the PI_{ABS} values of *A.*

arenaria and *G. pernambucencis* remained unaffected during the rainy and dry seasons (Fig. 4a, b). PI_{TOTAL} increased in *A. arenaria* at RBC by 74% and 16% during the rainy and dry seasons, respectively, compared to the reference. However, PI_{TOTAL} remained unaffected in *G. pernambucencis* at RBC during both seasons.

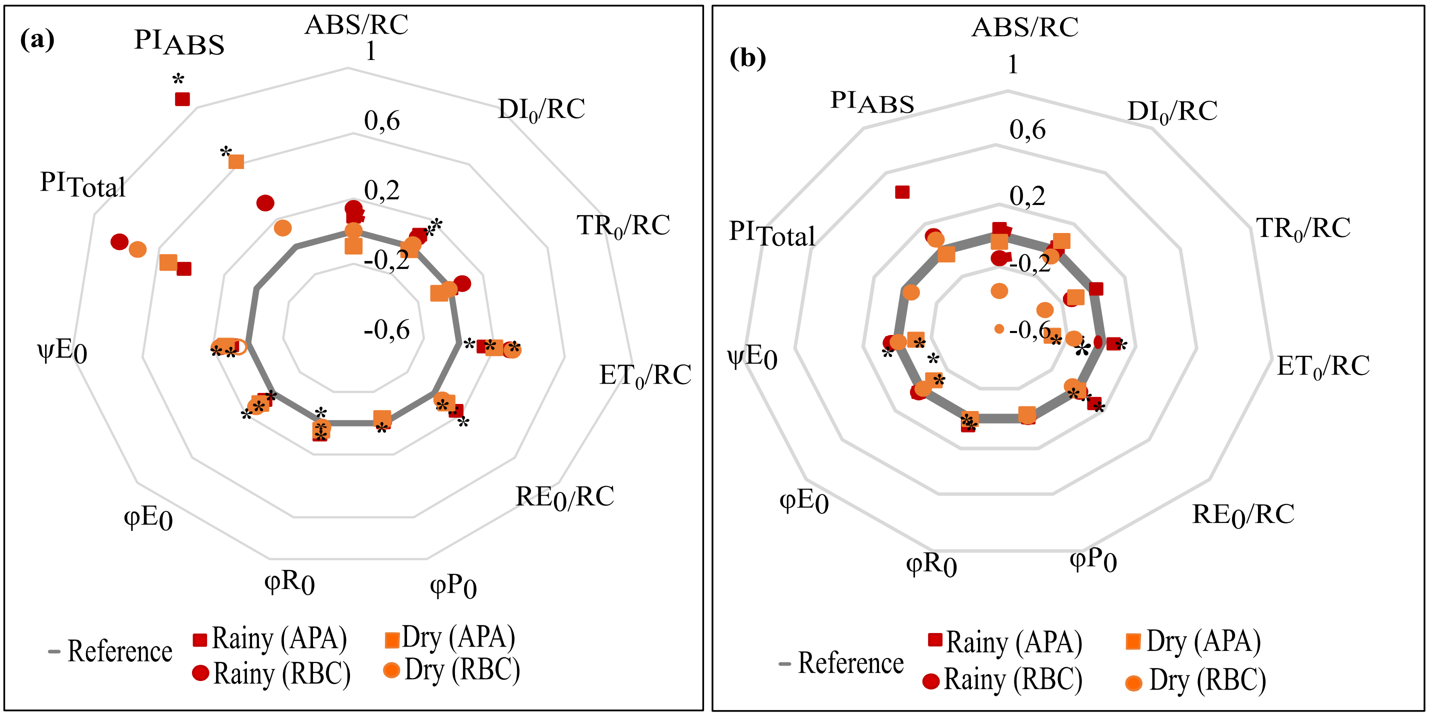

Fig. 4 Selected JIP parameters for *A. arenaria* (**a**) and *G. pernambucencis* (**b**) at the Environmental Protection Area of Conceição da Barra (APA) and the Comboios Biological Reserve (RBC). The JIP parameter values were normalized to those of the reference, which corresponded to samples collected from APA and RBC in February 2019. Asterisk (*) ($P < 0.05$) indicated a significant difference between the reference and the seasonal periods, as determined by the Tukey test.

Cluster analysis

The results of the cluster analysis of chlorophyll *a* fluorescence (ChlF) parameters are shown in Figure 5. A cluster analysis performed on the basis of all tested parameters, separated the 12 treatments with two sites x two species × three periods into six different clusters, with a cut-off point of a Euclidean distance 0.02. Cluster 1 contained the species *A. arenaria* at APA and RBC during the rainy season. The second cluster contained both species at RBC during the dry season. The third cluster included *A. arenaria* at APA during the dry season, *G. pernambucencis* at APA for all periods observed and *G. pernambucencis* at RBC for the reference period. Cluster 4, 5 and 6 contained *A. arenaria*, during the reference period, *G. pernambucencis* at RBC during the dry season and *A. arenaria* at APA during the reference period.

The lowest distance between cluster 1 and cluster 2 indicated that the smallest changes from rainy to dry seasons are observed in *A. arenaria*. However, the distance between *A. arenaria* at RBC during the reference period and *A. arenaria* at RBC during the other seasons was slightly higher. These results validate the results obtained through PCA, demonstrating a significant correlation between the concentrations of heavy metals in *A. arenaria* at RBC during the rainy season and soil pH (Fig. 1).

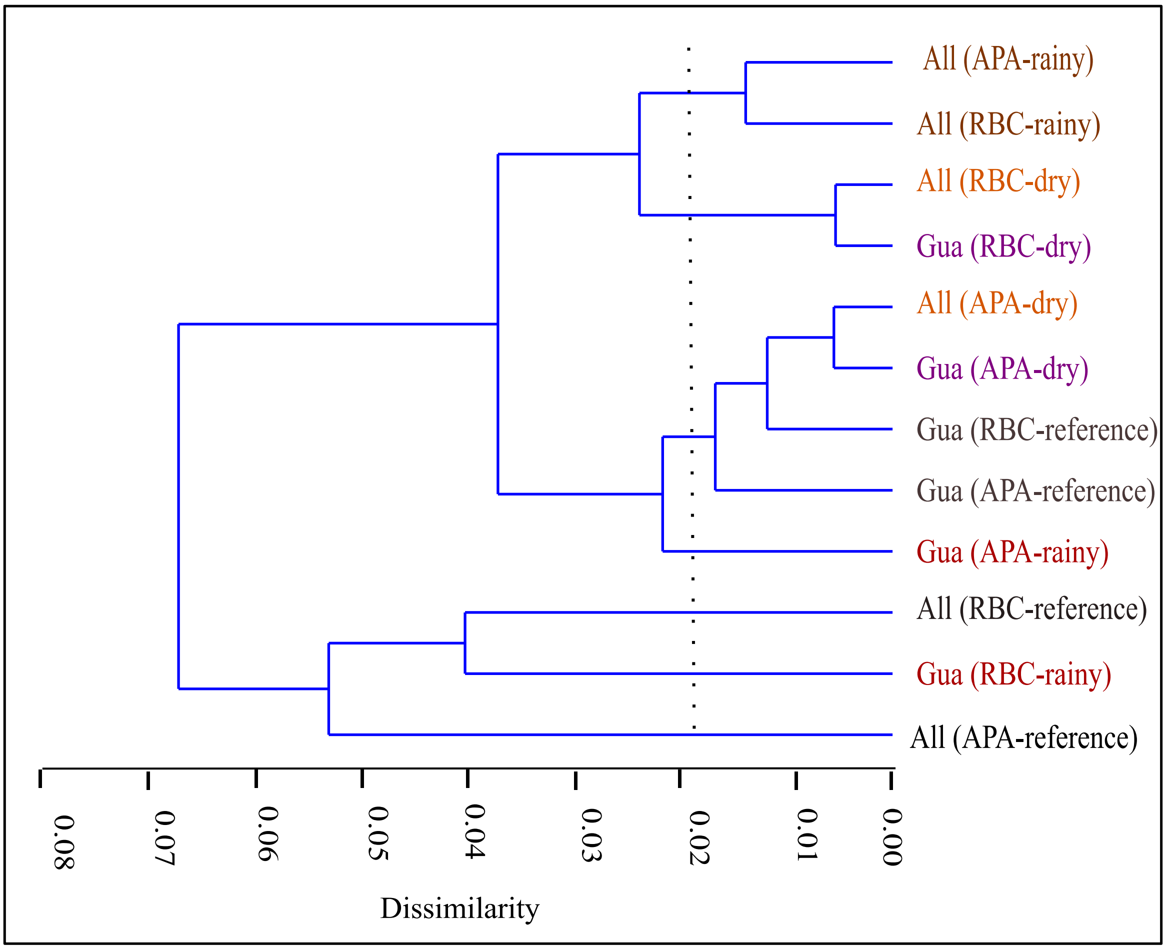

Fig. 5 Cluster analysis of fluorescence parameters for *A. arenaria* (All) and *G. pernambucencis* (Gua) at the Environmental Protection Area of Conceição da Barra (APA) and the Comboios Biological Reserve (RBC) in 2019 (reference point), 2020 (rainy season), and 2021 (dry season). Dendrograms were built using the UPGMA agglomeration method.

Discussion

The Environmental Protection Area of Conceição da Barra (APA) and the Comboios Biological Reserve (RBC) share similar physical soil properties, including high sand content (over 95%), weak acidity, and low organic matter content (OM). In contrast, a noticeable base saturation (V%) gradient was observed between APA and RBC. The texture of both soils corresponds to Neossolo quartzarênico soils, as proposed by Santos (2018), representing the typical soil type of the restinga region. Soil texture was identified as the most important environmental driver of coastal Atlantic Forest diversity, with the differentiation of restinga plant communities primarily influenced by organic content (Bona et al. 2020; Lourenço Júnior et al. 2021). RBC showed average base saturation (V%) results as the main fertility indicators of nutrient supply from the soil that are essential for plant growth, such as P, K, $Ca^{2+}$and Mg^{2+} (Lourenço et al. 2021; Barrow et al 2023; Rusconi et al. 2023). RBC possesses a favorable conservation status without agricultural activities, which may have contributed to the soil fertility at this site. Soil fertility can be an important indicator of forest recovery for plant communities affected by tailings (Ferreira et al. 2021; Fortes et al. 2022). Our results revealed that the V% in the soil was the primary driver in scrub restinga areas, suggesting that V% could serve as a crucial indicator for the recovery of plant communities affected by the tailings.

Researchers indicated that tailings from the dam rupture caused an increase in silt and clay in the Doce River estuary (Viana et al. 2020; Sá et al. 2021). Differently, silt and clay content were considered low (below 3% and 5%, respectively) at APA and RBC for all observed periods. Six years after the dam rupture, soil textures at APA and RBC were unaffected by changes in the granulometric fractions of the tailings from the Fundão Dam. RBC is located closer to the Doce River mouth, which may have been more affected by the tailings from the Fundão Dam. Researchers indicated that areas affected by the tailings showed elevated levels of Fe, Cd, and Mg (Viana et al. 2020; Duarte et al. 2021; Fernandes et al. 2022). Soil of the restinga herbaceous physiognomy exhibited a gradual reduction in heavy metal levels from the most distant areas to the ones closest to the Doce River mouth (Lana-Costa et al. 2021). However, there was no significant difference between the RBC and APA areas regarding metal concentrations in the soil, indicating that the distance from the river mouth is not a factor impacting metal accumulation in the evaluated areas. Davila et al. (2020) detected values of Ni (9.3 mg kg^{-1}), Cr (79 mg kg^{-1}), Mn (600 mg kg^{-1}), Cu (4.8 mg kg^{-1}), and V (17.4 mg kg^{-1}) from samples collected at the Fundão dam, which were higher than those found in the APA and RBC soil.

The increase in the uptake of As, Pb, and V by *A. arenaria* was observed at RBC during the rainy season compared to the reference period, even though the soil had low concentrations of these metals. The accumulation of heavy metals in plants depends on the mobility of the elements in the soil and the absorption capacity of each species (Dubey et al. 2018). Moreover, the deposition of salt spray can be a primary source of the spread of contaminated particles in coastal regions (Du and Hesp 2020; Lana-Costa et al. 2021; Oliveira et al. 2022). The primary origin of salt spray is commonly attributed to the bursting of bubbles in breaking waves, often recognized as a crucial factor influencing vegetation zonation in coastal dunes (Du and Hesp 2020). The collapse of the dam resulted in the dispersion of sediments from the Doce River over a vast area along the coast, covering hundreds of kilometers, which was primarily caused by the effects of the salt spray (Marta-Almeida et al. 2016; Duarte et al. 2021; Fortes et al. 2022). The primary factor responsible for the southward dispersion of the salt spray was the wind, which is a predictable occurrence in this region due to the seasonal variability in wind direction, with a predominance towards the south during the austral spring and summer (Marta-Almeida et al. 2016). The increase in heavy metal uptake by *A. arenaria* during the rainy season can also be explained by the salt spray. Following rainfall-runoff events, the mud that had settled within the river-estuary system was consistently leached, resulting in elevated levels of turbidity and extensive plumes spreading throughout the coastal area (Rudorff et al. 2018). These heavy metal dispersion processes are classified as diffuse pollution, since a significant portion of the sediment particles transported by water during heavy rainfall events have a low density and can remain suspended in the water (Dubey et al. 2018).

Changes in the F_0 and F_m values can influence the shape of the O-J phase, whose configuration demonstrates the photochemical reduction of Q_A and partial reoxidation of Q_A^- through PQ (via Q_B) (Tsimilli-Michael 2020). For example, the significant decrease in the J phases on the OJIP curve indicated the toxicity of the heavy metals, specifically Cd, in *Broussonetia papyrifera* (Zhang et al. 2020). Differently, the increased uptake of heavy metals did not significantly impair the ChlF emission in *A. arenaria*. The O-J phase remained stable, and no noticeable K-step appeared in any of the OJIP curves of either species. The O-J phase decrease can also indicate the irreversible damage to PSII, associated with light-harvesting complex II (LHCII), affecting the electron transfer on the reduced side of PSII (Singh et al. 2022). This is further supported by results from ABS/RC, TR_0/RC and DI_0/RC parameters which are obtained from the O-J phase and express the specific energy fluxes per active reaction center. ABS/RC is considered as a measure for apparent antenna size or chlorophyll concentration and TR_0/RC reflects the specific rate of the exciton trapped by reaction centers (Tsimilli-Michael 2020). Excessive levels of Mn, Cu, and Fe showed a strong correlation with the increased DI_0/RC in *Melia azedarach* and *Byrsonima sericea* (Liu et al. 2021; Oliveira et al. 2022). Thus, the total amount of photons absorbed by Chl molecules and the activity of active RCs remain unaffected in *A. arenaria* at RBC during the rainy season, which demonstrated that the high levels of As, V and Pb did not cause severe disruption to leaf photosynthetic organs and oxygen-evolving complex functionality (OEC) damage. ΔWOI also remained stable for *A. arenaria* at RBC during the rainy. ΔWOI serves to distinguish the sequence of events from exciton trapping by PS II up to plastoquinone (PQ) reduction (Yusuf et al. 2010). Therefore, this may indicate that the increase in the concentration of As, Pb, and V in leaves of *A. arenaria* at RBC during the rainy did not affect the initial rate of active PSII reaction centers closure.

Heavy metals mainly affect the electron transfer process in photosystem I (PSI) of chloroplasts (Kalaji et al. 2016; Małkowski et al. 2019; Bussotti et al. 2020; Liu et al. 2021). The J-I phase represents the decline in the amounts of intersystem electron carriers Q_B, PQ, and Cyt b_6/f, which are determined by their sizes (especially PQ) and the speed of subsequent reactions (Tsimilli-Michael 2020). For example, significantly increases in the J–I phase were seen by Mn stress in *M. azedarach*, which represented a change in the PQ pool (Liu et al. 2021). *Nicotiana tabacum* with elevated Pb levels exhibited a reduction in the I-P phase of the OJIP curve, indicating the inactivation of the PSI acceptor side or inhibition in the electron transport from the donor side of PSII to the acceptor side of PSI (Kalaji et al. 2016). The I-P phase reflects a reduction in PC^+, $P700^+$, and PSI end electron acceptors (RE) using electrons from PQH_2, which is facilitated by PSI activity (Tsimilli-Michael 2020). However, our results show that the J–I phase decreased and I–P phase remained unaffected in *A. arenaria* during the rainy season, which may indicate that the increase in metal concentrations of at RBC did not affect PSI. This is further supported by results from PI_{TOTAL} parameters, that increased in *A. arenaria* at RBC during the rainy season. Previous studies showed that increases in heavy metal concentrations can also affect the parameters associated with maximum quantum PSII (φP_0) efficiency, electron flux beyond Q_A^- (φE_0) and the electron flux to PSI end electron acceptors (φR_0) (Małkowski et al. 2019; Liu et al. 2021). For example, the φP_0 parameter decreases in *Arabidopsis thaliana* and *Arabidopsis helleri* under Cd stress, with excess Mn, damaged PSII activity (Małkowski et al. 2019). The φR_0 and φP_0 parameter also decreased in *P. australis* exposed to excess Pb. The reduction of φP_0 and φR_0 reflected the damage to the PSII activity and decreased PSI capacity by reducing ferredoxin and $NADP^+$ (Liu et al. 2021). The φR_0 and φP_0 parameters were enhanced in *A. arenaria,* when metal concentrations increased at RBC. High φP_0 values indicated that most of the absorbed light energy was utilized for photochemical reactions, while the increase in φR_0 suggested that a significant portion of the absorbed light energy was being dissipated as heat or fluorescence (Tsimilli-Michael 2020).

The impact of precipitation deficits on photochemical efficiency can be evaluated by the PI_{ABS} parameter, which is the performance index for energy conservation from photons absorbed by PSII resulting in a reduction of intersystem electron acceptors (Goltsev et al. 2016). Drought damages the photochemical apparatus in restinga species (Silva et al. 2017; Lana-Costa et al. 2021; Oliveira et al. 2022). *B. sericea* exhibited reduced φP_0 and PI_{ABS} values during the dry season, which may have resulted from the inactivity of the RCs (Oliveira et al. 2022). Severe drought stress also led to a decrease in the φP_0 in a sensitive genotype of *Triticum sp* (Barboričová et al. 2020). Low φP_0 showed a strong correlation with a decrease in PI_{ABS}, which is considered a sensitive indicator of water stress (Barboričová et al. 2020; Oliveira et al. 2022; Souza et al. 2022). On the other hand, the φP_0 of a drought-resistant cultivar of *Coffea arabica* was minimally affected, demonstrating the integration between PSII and PSI (Dubberstein et al. 2020). Our study demonstrated that φP_0 and PI_{ABS} remained unaffected in *A. arenaria* and *G. pernambucensis* during the dry season. According to the cluster analysis, ChlF emission in both species remained stable during the dry season, which could be associated with the stability of the JIP test during drought periods. Furthermore, the analysis of ChlF parameters was more sensitive to variations in heavy metals within plant tissues. This suggests that the increased overall activity of PSII is primarily a result of enhanced energetic connectivity between PSII units and OEC state, along with greater efficiency in electron transport through PSII (Tsimilli-Michael 2020). The results demonstrated that two shrubs species have different strategies to cope with excess metal in the soil. The different physiological responses of *A. arenaria* and *G. pernambucencis* to heavy metals could be considered as an acclimation strategy. Our results confirmed the hypothesis that changes in soil fertility affected the concentrations of metals in *A. arenaria* and *G. pernambucensis*. However, an increase in the concentrations of metals in either species under different precipitation regimes did not cause severe damage to chlorophyll *a* fluorescence.

Conclusions

A. arenaria and *G. pernambucensis* exhibit photochemical in response to increased to heavy metals that indicated the presence of potential tolerance mechanisms. These findings could help understand the effect of mine tailings over a range of situations, from local to global. As, Pb, and V were absorbed by *A. arenaria*, which demonstrated an acclimation strategy to the increased absorption of heavy metals. The parameters related to quantum yield (φE_0, φP_0, φR_0) and PI_{TOTAL} efficiently demonstrated the differential photochemical efficiency of *A. arenaria* in response to increased absorption of heavy metals. Adjustments in the test parameters such as increased φR_0 and $\varphi P_{0,}$ were associated to acclimation of the photochemical apparatus to increases in heavy metal concentrations. The increase in PI_{Total} values observed exclusively in *A. arenaria* during the dry season may indicate a more efficient tolerance mechanisms than those seen in *G. pernambucensis*. In conclusion, this research demonstrates that chlorophyll *a* fluorescence is a rapid and precise tool that facilitates the comprehension of the long-term impacts of heavy metals on natural ecosystems following the failure of a mining dam, such as the Fundão dam. Further analyses, encompassing plant anatomy, secondary metabolites, and antioxidant enzymes, are essential to elucidate the interplay between physiological changes and the enduring adaptive effects of heavy metals on restinga vegetation.

Acknowledgments: The authors would like to express their gratitude to the administration of Comboios Biological Reserve, NEF laboratory, and the VIES herbarium for their support during this study. Additionally, the authors extend their thanks to the Coordenação de Aperfeiçoamento de Pessoal de Nível Superior – Brasil (CAPES) for providing a research fellowship to N.G.M.L.

Authors' Contributions: N.G.M.L and D.M.S conceived the ideas and designed the methodology. N.G.M.L collected and analyzed the data and drafted the initial manuscript. D.M.S, M.G.C.F, and E.C reviewed the paper. All authors made substantial contributions to the manuscript and approved the final version.

Funding This study received partial financial support from the Biological Diversity Monitoring Program (PMBA) of the Rede Rio Doce Mar, as established by the Technical-Scientific Agreement (DOU number 30/2018) between FEST (Fundação Espírito-santense de Tecnologia) and the Renova Foundation.

Data Availability The datasets from the current study are available from the corresponding author upon request.

Conflict of Interest The authors declare that they have no conflicts of interest.

Reference

Barrow NJ, Hartemink AE (2023) The effects of pH on nutrient availability depend on both soils and plants. Plant and Soil 487: 21–37. https://doi.org/10.1007/s11104-023-05960-5

Barboričová M, Filaček A, Vysoká DM, Gašparovič K, Živčák M, Brestic M (2022) Sensitivity of fast chlorophyll fluorescence parameters to combined heat and drought stress in wheat genotypes. Plant, Soil and Environment, 68(7), 309-316. https://doi.org/10.17221/87/2022-PSE

Bechara FC, Salvador LZ, Ventura RA, Topanotti LR, Gerber D, Cruz IS, Simonelli M (2020) Vegetation and seed bank of an open-scrub bush restinga formation in the Southeastern coast of Brazil. Revista de Biología Tropical, 68(2), 541-550. http://dx.doi.org/10.15517/rbt.v68i2.39241

Bona C, Pellanda RM, Carlucci MB, Machado RGP, Ciccarelli D (2020) Functional traits reveal coastal vegetation assembly patterns in a short edaphic gradient in southern Brazil. Flora, 271, 151661. https://doi.org/10.1016/j.flora.2020.151661

Brito LS, Irmler U, Forte BVG, Xavier TP, Martins RL (2018) Matter turnover in the oligotrophic restinga ecosystem and the importance of the key species *Clusia hilariana*. Biota Neotrop 18:1–10. https://doi.org/10.1590/1676-0611-BN-2018-0552

Bussotti F, Gerosa G, Digrado A, Pollastrini M (2020) Selection of chlorophyll fluorescence parameters as indicators of photosynthetic efficiency in large scale plant ecological studies. Ecol Indic 108:105686. https://doi.org/10.1016/j.ecolind.2019.105686

https://doi.org/10.1016/S0065-2113(06)91003-7Cruz FVS, Gomes MP, Bicalho EM, Della TF, Garcia QS (2020) Does Samarco's spilled mud impair the growth of native trees of the Atlantic Rainforest? Ecotoxicol Environ Saf 189:110021. https://doi.org/10.1016/j.ecoenv.2019.110021

Dalotto CES, Sühs RB, Dechoum MS, Pugnaire FI, Peroni N, Castellani TT (2018) Facilitation influences patterns of perennial species abundance and richness in a subtropical dune system. AoB Plants 10(2):1-8. . https://doi.org/10.1093/aobpla/ply017

Davila RB, Fontes MPF, Pacheco AA, Ferreira MS (2020) Heavy metals in iron ore tailings and floodplain soils affected by the Samarco dam collapse in Brazil. Science of the Total Environment 709:136151. https://doi.org/10.1016/j.scitotenv.2019.136151

Du J, Hesp PA (2020) Salt Spray Distribution and Its Impact on Vegetation Zonation on Coastal Dunes: a Review. Estuaries and Coasts 43:1885–1907. https://doi.org/10.1007/s12237-020-00820-2

Duarte EB, Neves MA, Oliveira FB, Martins ME, Oliveira CHR, Burak DL, Orlando MTDA, Rangel CVGT (2021) Trace metals in Rio Doce sediments before and after the collapse of the Fundão iron ore tailing dam, Southeastern Brazil. Chemosphere 262:127879. https://doi.org/10.1016/j.chemosphere.2020.127879

Dubberstein D, Lidon FC, Rodrigues AP, Semedo JN, Marques I, Rodrigues WP, Gouveia D, Armengaud J, Semedo MC, Martins S, Simões-Costa MC, Moura I, Pais IP, Scotti-Campos P, Partelli FL, Campostrini E, Ribeiro-Barros AI, DaMatta FM, Ramalho JC (2020) Resilient and Sensitive Key Points of the Photosynthetic Machinery of *Coffea spp.* to the Single and Superimposed Exposure to Severe Drought and Heat Stresses. Front. Plant Sci. 11:1049. https://doi.org/10.3389/fpls.2020.01049

Dubey S, Shri M, Gupta A, Rani V, Chakrabarty D (2018) Toxicity and detoxification of heavy metals during plant growth and metabolism. Environ Chem Lett 16:1169–1192. https://doi.org/10.1007/s10311-018-0741-8

Fernandes L, Jesus H, Almeida P, Sandrini J, Bianchini A, Santos H (2022) The influence of the Doce River mouth on the microbiome of nearby coastal areas three years after the Fundão Dam failure, Brazil. Science of the Total Environment 807:151777. https://doi.org/10.1016/j.scitotenv.2021.151777

Ferreira GWD, Ribeiro BT, Weindorf DC, Teixeira BI, Chakraborty S, Li B, Guilherme LRG, Scolforo JRS (2021) Assessment of iron-rich tailings via portable X-ray fluorescence spectrometry: the Mariana dam disaster, southeast Brazil. Environ Monit Assess 193. https://doi.org/10.1007/s10661-021-08982-7

Flora do Brasil Jardim Botânico do Rio de Janeiro. URL: http://floradobrasil.jbrj.gov.br/. Accessed 28 June 2023 (in Portuguese)http://floradobrasil.jbrj.gov.br/

Fortes BCS, Teixeira MCV, Costa SP, Wagner MH, Scotti, MR (2022) Post-disaster recovery plan for a rural settler's community affected by the Fundão dam tailings in Brazil. J Rural Stud 93:55–66. https://doi.org/10.1016/j.jrurstud.2022.05.013

Ghori NH, Ghori T, Hayat M Q, Imadi SR, Gul A, Altay V, Ozturk M (2019) Heavy metal stress and responses in plants. International Journal of Environmental Science and Technology 16:1807–1828. https://doi.org/10.1007/s13762-019-02215-8

Goltsev VN, Kalaji HM, Paunov M, Bąba W, Horaczek T, Mojski J (2016) Variable chlorophyll fluorescence and its use for assessing physiological condition of plant photosynthetic apparatus. Russ J Plant Physiol. 63(1):869-93. https://doi.org/10.1134/S1021443716050058

Hanelt D (2018) Photosynthesis assessed by chlorophyll fluorescence. In; Häder DP, Erzinger GS (eds) Bioassays: Advanced Methods and Applications. Elsevier, pp169–198. https://doi.org/10.1016/B978-0-12-811861-0.00009-7

Huang CYL, Schulte EE (1985) Digestion of Plant Tissue for Analysis by ICP Emission Spectroscopy. Commun Soil Sci Plant Anal 16:943–958. https://doi.org/10.1080/00103628509367657

https://doi.org/10.1016/j.envexpbot.2017.11.001Kalaji HM, Jajoo A, Oukarroum A, Brestic M, Zivcak M, Samborska IA, Cetner MD, Łukasik I, Goltsev V, Ladle RJ (2016) Chlorophyll a fluorescence as a tool to monitor physiological status of plants under abiotic stress conditions. Acta physiologiae plantarum, *38*, 1-11. https://doi.org/10.1007/s11738-016-2113-y

Khan A, Khan S, Khan MA, Qamar Z, Waqas M (2015). The uptake and bioaccumulation of heavy metals by food plants, their effects on plants nutrients, and associated health risk: a review. Environmental science and pollution research, 22, 13772-13799. https://doi.org/10.1007/s11356-015-4881-0

Lana-Costa J, Silva MM, Martins AO, Guarnier JC et al (2021) Biochemical and physiological aspects of restinga herbaceous plants tolerance to iron ore tailing plume along the coastal region of Espírito Santo-Brazil. Environ. Exp. Bot. 191:104618. https://doi.org/10.1016/j.envexpbot.2021.104618

Liu MS, Huang X.H, Wang R.J, Xu HY, Zhu F (2021) Inhibition of photosynthesis in *Melia azedarach* and *Ligustrum lucidum* induced by manganese toxicity using OJIP chlorophyll a fluorescence transient. *Photosynthetica* 59: 148–159. https://doi.org/ 10.32615/ps.2021.006

Lourenço Júnior J, Newman EA, Ventura JA, Milanez CRD et al (2021) Soil-associated drivers of plant traits and functional composition in Atlantic Forest coastal tree communities. Ecosphere 12(7):03629. https://doi.org/10.1002/ecs2.3629

Lysenko EA, Klaus AA, Kartashov A V,Kusnetsov VV (2020) Specificity of Cd, Cu, and Fe effects on barley growth, metal contents in leaves and chloroplasts, and activities of photosystem I and photosystem II. Plant Physiology and Biochemistry 147, 191–204. https://doi.org/10.1016/j.plaphy.2019.12.006

Małkowski E, Sitko K, Zieleźnik-Rusinowska P, Gieroń Ż, Szopiński M (2019) Heavy metal toxicity: Physiological implications of metal toxicity in plants. In Sablok, G. (eds) Plant Metallomics and Functional Omics: A System-Wide Perspective. Springer International Publishing, pp. 253–301

Marta-Almeida M, Mendes R, Amorim FN, Cirano M, Dias JM (2016) Fundão Dam collapse:Oceanic dispersion of River Doce after the greatest Brazilian environmental accident. Mar Pollut Bull 112: 359–364. https://doi.org/10.1016/j.marpolbul.2016.07.039

Menezes AR, Fontana A, Anjos LHC (2018) Spodosols in Brazil: distribution, characteristics and diagnostic attributes of spodic horizons. *S*outh African Journal of Plant and Soil 35:241–250. https://doi.org/10.1080/02571862.2017.1410734

Monteiro MM, Giaretta A, Pereira OJMenezes LFT (2014) Composição e estrutura de uma restinga arbustiva aberta no norte do Espírito Santo e relações florísticas com formações similares no Sudeste do Brasil. Rodriguésia 1:65–72 (in Portuguese). https://doi.org/10.1590/S2175-78602014000100005

Nivelais L, Levallois A, Basuyaux O, Costil K, Lebel JM, Larsonneur S, Guichard G, Serpentini A, Caplat C. (2023) Effects on growth of juvenile abalones haliotis tuberculata under chronic exposition to metals released from the dissolution of an aluminium-based galvanic anode. Archives of Environmental Contamination and Toxicology, 84(1), 32-44. https://doi.org/10.1007/s00244-022-00975-y

Oliveira GC, Broetto SG, Pereira OJ, Penha JS, Lopes NGM, Silva DM (2022) Effects of different levels of metal exposure and precipitation regimes on chlorophyll *a* fluorescence parameters in a coastal Brazilian restinga species. J Photochem Photobiol 12: 100153. https://doi.org/10.1016/j.jpap.2022.100153

Pandey P, Ramegowda V, Senthil-kumar M (2015) Shared and unique responses of plants to multiple individual stresses and stress combinations: physiological and molecular mechanisms. Frontiers in Plant Science 6:1–14. https://doi.org/10.3389/fpls.2015.00723

Prezotti AGM, Guarçoni MA (2013). Guia de interpretação de análise de solo e foliar (in Portuguese) Incaper, Vitória

Rudorff N, Rudorff CM, Kampel MOG (2018) Remote sensing monitoring of the impact of a major mining wastewater disaster on the turbidity of the Doce River plume off the eastern Brazilian coast. ISPRS Journal of Photogrammetry and Remote Sensing 145:349–361. https://doi.org/10.1016/j.isprsjprs.2018.02.013

Rusconi O, Steiner T, Bayon C, Rasmann S (2023) Soil properties and plant species can predict population size and potential introduction sites of the endangered orchid *Cypripedium calceolus*. Plant and Soil 487:467–483. https://doi.org/10.1007/s11104-023-05945-4

Sá F, Longhini CM, Costa ES, Silva CA,Cagnin RC, Gomes LEO, Lima AT, Bernardino AF, Rodrigues Neto R (2021) Time-sequence development of metal(loid)s following the 2015 dam failure in the Doce river estuary, Brazil. Science of the Total Environment 769:1–12. https://doi.org/10.1016/j.scitotenv.2020.144532

Santos HG, Jacomine PKT, Anjos LHC, Oliveira VA, Lumbreras JF, Coelho MR.; Almeida JA, Araujo Filho JC, Oliveira JB, Cunha TJF (2018) Brazilian Soil Classification System (in Portuguese). 5 ed. Embrapa, Brasília

Santos-Filho FS, Almeida EB, Zickel CS (2013) Do edaphic aspects alter vegetation structures in the Brazilian restinga? Acta Bot Brasilica 27:613–623. https://doi.org/10.1590/S0102-33062013000300019

Scarano FR, (2002) Structure, function and floristic relationships of plant communities in stressful habitats marginal to the Brazilian Atlantic rainforest. Ann Bot 90: 517–524. https://doi.org/10.1093/aob/mcf189

Silva LC, Araújo TO, Martinez CA, Lobo AF, Azevedo AA,Oliva MA (2015) Differential responses of C3 and CAM native Brazilian plant species to a SO_2- and SPM_{Fe}-contaminated Restinga. Environmental Science and Pollution Research 22: 14007–14017. https://doi.org/10.1007/s11356-015-4391-0

Silva LC, Araújo TO, Siqueira-Silva AI, Pereira TAR, Castro LN, Silva EC, Oliva MA, Azevedo A.A (2017) *Clusia hilariana* and *Eugenia uniflora* as bioindicators of atmospheric pollutants emitted by an iron pelletizing factory in Brazil. Environmental Science and Pollution Research, 24, 28026-28035. https://doi.org/10.1007/s11356-017-0386-3

Singh H, Kumar D, Soni V (2022) Performance of chlorophyll a fluorescence parameters in *Lemna minor* under heavy metal stress induced by various concentration of copper. Sci Rep 12: 10620. https://doi.org/10.1038/s41598-022-14985-2

Souri Z, Cardoso AA, Silva CJ, Oliveira LM., Dari B, Sihi D, Karimi N (2019) Heavy metals and photosynthesis: Recent developments. In: Ahmad P., Ahanger MA, Alyemeni MN, Alam P (Eds) Photosynthesis, productivity and environmental stress, Wiley, New York, pp 107–134

Stirbet A, Lazár D, Kromdijk J, Govindjee (2018) Chlorophyll a fluorescence induction: Can just a one-second measurement be used to quantify abiotic stress responses? Photosynthetica 56:86–104. https://doi.org/10.1007/s11099-018-0770-3

Tognella MMP, Falqueto AR, Espinoza HDCF, Gontijo I, Gontijo ABPL, Fernandes AA, Schmildt ER, Soares MLG, Chaves FO, Schmidt AJ, Lopes DS, Barcelos UD, D'Addazio V, Lima KOO, Pascoalini SS, Paris JO, Brites-Júnior NV, Porto LA, Almeida-Filho E, Oliveira CP, Leopoldo RVS, Leite S, Berribilli MP, Ronconi SFV, Rosa MB, Sá F, Rodrigues-Neto R, Ghisolfi RD, Castro MSM, Rigo D, Tosta VC, Albino J(2022) Mangroves as traps for environmental damage to metals: The case study of the Fundão Dam. Science of the Total Environment 806: 150452. https://doi.org/10.1016/j.scitotenv.2021.150452

Tsimilli-Michael M (2020) Revisiting JIP-test: An educative review on concepts, assumptions, approximations, definitions and terminology. Photosynthetica 58: 275–292. https://doi.org/10.32615/ps.2019.150 http://dx.doi.org/10.32615/ps.2019.150http://dx.doi.org/10.32615/ps.2019.150

Viana LMS, Pestana IA, Carvalho CEV, Salomão MSMB (2020) Doce River Estuary: Geochemical Changes Following the Largest Tailing Spill in South America. Arch Environ Contam Toxicol 79:343–353. https://doi.org/10.1007/s00244-020-00766-3

Yusuf MA, Kumar D, Rajwanshi R., Strasser R J, Tsimilli-Michael M, Govindjee, Sarin NB (2010) Overexpression of γ-tocopherol methyl transferase gene in transgenic *Brassica juncea* plants alleviates abiotic stress: Physiological and chlorophyll a fluorescence measurements. Biochim Biophys Acta Bioenerg 1797: 11428–1438. https://doi.org/10.1016/j.bbabio.2010.02.002

Zhang W, Zhao Y, Xu Z, Huang H, Zhou J,Yang G. (2020) Morphological and physiological changes of *Broussonetia papyrifera* seedlings in cadmium contaminated soil. Plants 9:1–17. https://doi.org/10.3390/plants9121698